BJR

Received: 19 October 2015 | Revised: 18 February 2016 | Accepted: 24 February 2016

http://dx.doi.org/10.1259/bjr.20150870

Cite this article as:
Yoganathan SA, Maria Das KJ, Mohamed Ali S, Agarwal A, Mishra SP, Kumar S. Evaluating the four-dimensional cone beam computed tomography with varying gantry rotation speed. *Br J Radiol* 2016; **89**: 20150870.

FULL PAPER

Evaluating the four-dimensional cone beam computed tomography with varying gantry rotation speed

[1]S A YOGANATHAN, MSc, [1]K J MARIA DAS, PhD, [2]SHAJAHAN MOHAMED ALI, MSc, [1]ARPITA AGARWAL, MSc, [2]SURENDRA P MISHRA, PhD and [1]SHALEEN KUMAR, MD

[1]Deparment of Radiotherapy, Sanjay Gandhi Post-graduate Institute of Medical Sciences, Lucknow, Uttar Pradesh, India
[2]Department of Radiation Oncology, Dr Ram Manohar Lohia Institute of Medical Sciences, Lucknow, Uttar Pradesh, India

Address correspondence to: Mr S A Yoganathan
E-mail: *sayoganathan@yahoo.co.in*

Objective: The purpose of this work was to evaluate the four-dimensional cone beam CT (4DCBCT) imaging with different gantry rotation speed.
Methods: All the 4DCBCT image acquisitions were carried out in Elekta XVI Symmetry™ system (Elekta AB, Stockholm, Sweden). A dynamic thorax phantom with tumour mimicking inserts of diameter 1, 2 and 3 cm was programmed to simulate the respiratory motion (4 s) of the target. 4DCBCT images were acquired with different gantry rotation speeds (36°, 50°, 75°, 100°, 150° and 200° min^{-1}). Owing to the technical limitation of 4DCBCT system, average cone beam CT (CBCT) images derived from the 10 phases of 4DCBCT were used for the internal target volume (ITV) contouring. ITVs obtained from average CBCT were compared with the four-dimensional CT (4DCT). In addition, the image quality of 4DCBCT was also evaluated for various gantry rotation speeds using Catphan® 600 (The Phantom Laboratory Inc., Salem, NY).
Results: Compared to 4DCT, the average CBCT underestimated the ITV. The ITV deviation increased with increasing gantry speed (−10.8% *vs* −17.8% for 36° and 200° min^{-1} in 3-cm target) and decreasing target size (−17.8% *vs* −26.8% for target diameter 3 and 1 cm in 200° min^{-1}). Similarly, the image quality indicators such as spatial resolution, contrast-to-noise ratio and uniformity also degraded with increasing gantry rotation speed.
Conclusion: The impact of gantry rotation speed has to be considered when using 4DCBCT for ITV definition. The phantom study demonstrated that 4DCBCT with slow gantry rotation showed better image quality and less ITV deviation.
Advances in knowledge: Usually, the gantry rotation period of Elekta 4DCBCT system is kept constant at 4 min (50° min^{-1}) for acquisition, and any attempt of decreasing/increasing the acquisition duration requires careful investigation. In this study, the 4DCBCT images with different gantry rotation speed were evaluated.

INTRODUCTION

Advancements in radiotherapy resulted in intensity-modulated radiation therapy, which enabled us to sculpt the radiation dose distribution tightly around the tumour while sparing the critical organs.[1] The high dose conformity requires better targeting accuracy, but it is hampered by organ motions in many sites, and the organ motions are classified into intrafractional and interfractional motions. These motions create geometric as well as dosimetric uncertainties in the radiotherapy treatment.[2–4]

The intrafractional tumour motions can be managed by motion encompassing,[5,6] breath-hold,[7] gating[8,9] or tracking[10–12] techniques. Among these, the motion encompassing method is the main focus of this work. In this method, an internal margin (IM) is added to clinical target volume to account for the physiological motion of tumour, and the clinical target volume plus IM defines the internal target volume (ITV).[5]

On the other hand, interfractional motions can be managed by in-room imaging devices such as gantry mounted cone beam CT (CBCT) systems.[13] CBCT imaging can be used for correcting interfractional motions and allows to localize the target prior to treatment delivery;[14,15] in addition, the CBCT images can also be used for adaptive radiotherapy planning.[16] Conversely, intrafractional respiratory motion limits the effective use of CBCT imaging in dynamic targets such as in the thoracic region. Respiratory motion creates artefacts in CBCT images, such as blurring, doubling, streaking and distortions, which greatly degrade the image quality and hence affect the target localization accuracy.[17–19]

Nowadays, the four-dimensional CT (4DCT) scan is increasingly used in clinics for radiotherapy planning of thoracic and upper-abdomen sites[20,21] owing to its superiority in eliminating the respiration-induced artefacts, which also enables a more accurate description of tumour motion. For a true four-dimensional (4D) treatment, ideally the verification imaging should also include a fourth dimension. Recently, the time synchronized CBCT (4DCBCT) method has been introduced to manage respiration-induced target motion during treatment verification imaging.[22–30] In 4DCBCT imaging, two-dimensional (2D) projections acquired at different times and positions are sorted into several groups, according to their respiratory phases, and each phase group is then reconstructed independently to obtain a volumetric image corresponding to that specific phase. The respiratory wave required for retrospective 4DCBCT reconstructions is derived using either 2D projections of CBCT itself or an external surrogate system.

The gantry rotation speed ($360° \text{ min}^{-1}$) of the usual three-dimensional cone beam CT acquisition technique may not be adequate for 4DCBCT acquisition because the large angular spacing would cause streak artefacts.[22–24] There are two methods discussed for reducing the angular spacing in 4DCBCT; one uses multiple rotations around the patient with normal gantry speed,[22,23] and the other uses reduced gantry speed (slow rotation).[23–25] It has been concluded that the slower gantry rotation produces superior 4DCBCT images compared with multiple gantry rotation since the multiple gantry rotation method may miss or duplicate projections.[23]

Li et al[22] developed a 4DCBCT technique in a commercially available On-Board Imaging system attached to a Varian® treatment machine (Varian Medical Systems, Palo Alto, CA). The CBCT projections were increased by using multiple-rotation scan, and the respiratory motion was measured using a small radio-opaque marker placed in the field of view of CBCT projections. The acquired 2D projections were sorted and reconstructed based on the respiratory phases.

Sonke et al[24] developed a respiratory-correlated CBCT method for acquiring 4D images in an Elekta linear accelerator (Elekta AB, Stockholm, Sweden). In this method, the CBCT data were acquired with slow gantry rotation, and the acquired 2D projection data were sorted and reconstructed retrospectively according to the respiratory phases. The respiratory wave required for retrospective reconstruction of 4DCBCT was derived from the 2D projection data, which eliminates the necessity of external surrogate system. Recently, Elekta commercialized this 4DCBCT method for imaging respiratory-induced moving targets. This 4DCBCT system allows visualizing the dynamic characteristics of tumours with reduced motion artefacts, enabling us to ensure the adequacy of IM in moving targets.

Previously, three-dimensional cone beam CT has been evaluated systematically for ITV definition, and the results are reported in literature.[31–33] However, 4DCBCT has not been analysed for ITV definition, especially for different gantry rotation speeds. Therefore, the purpose of this study was to evaluate the Elekta 4DCBCT system for deriving ITV with different gantry rotation speeds. The 4DCBCT ITVs were also compared with 4DCT ITVs. In addition, the effect of gantry rotation speed on 4DCBCT image quality was also evaluated.

The 4DCBCT system [XVI, v. 4.5 (Elekta AB)] used in this study did not allow exporting all 10 phases of 4DCBCT; therefore, the average CBCT derived from all the 10 4DCBCT phases were used for evaluation.

METHODS AND MATERIALS

Internal target volume analysis

4DCBCT acquisitions were carried out in Elekta X-ray volume imaging (XVI) Symmetry™ 4DCBCT system (v. 4.5) (Elekta AB) using phantom experiments. The CBCT scanner consists of an X-ray tube and a-Si flat-panel imager attached perpendicular to the megavoltage beam central axis with a common axis of rotation to megavoltage source. The maximum area of the detector is 25.6×25.6 cm at the isocentric plane with the pixel size of 512×512. The detector operates at a fixed frame rate of 5.5 frames per second while X-ray pulses are synchronized to the image acquisition such that the gantry rotation speed determines the number of projections per revolution. To acquire a volume, the gantry is rotated over 360° for a full scan and 195° for a half scan.

A dynamic thorax phantom Model 008A (CIRS, Norfolk, VA) with tumour mimicking spherical inserts of diameter 1, 2 and 3 cm was programmed to simulate the sinusoidal respiratory motion (regular) of the target. It was shown that the lung tumour motion is larger in craniocaudal (CC) direction (>10 mm) than both anteroposterior and right–left direction (approximately 2 mm), and the average respiratory motion period is approximately 4 s.[34] Therefore, the respiratory motion considered in this study was having the breathing period 4 s and amplitude 15 mm in CC, 2.5 mm in both anteroposterior and right–left direction. In order to generate a hysteresis motion pattern, a phase shift of 20% was used for both anteroposterior and right–left motions with respect to CC motion. A lung equivalent rod with the above spherical target sizes was put into the lung equivalent lobe of the phantom. This rod was connected to a motion actuator box for three-dimensional target motions.

The moving targets of different diameters were imaged by XVI using the default XVI Symmetry preset (120 kV; 20 nominal mA/frame; 16 nominal ms/frame). This preset has slow gantry rotation speed $50° \text{ min}^{-1}$ for 200° rotation with start and stop gantry angle 180° and 20° (in clockwise direction); the total scan duration was 4 min. Kilovoltage collimator and filter used during imaging were S20 and F0. The acquired 2D projection data were sorted retrospectively, which resulted in 10 groups of projections each corresponding to a particular respiratory phase. Finally, the sorted 2D projections were reconstructed (slice thickness 2 mm, pixel size 512×512) as 4D data set corresponding to 10 respiratory phases for visualization. In addition, the XVI also generated an averaged CBCT image set using these 10 CBCT phases (which only can be exported and not all the 10 phases). Similarly, additional 4DCBCT acquisitions were also carried out with same imaging parameters but different gantry speeds, such as 36°, 75°, 100°, 150° and $200° \text{ min}^{-1}$.

For the same moving targets, 4DCT acquisitions (2-mm slice thickness) were also carried out using a wide-bore multislice CT unit (SOMATOM® Sensation Open; Siemens Medical Systems, Erlangen, Germany). The 4DCT acquisitions were carried out in helical mode with the gantry rotation period of 0.5 s per rotation and pitch factor of 0.1. The Real-time Position Management™ system (Varian Medical Systems) was used to generate the respiratory wave of the moving target, and this wave was used for retrospective reconstruction of 4DCT images (2-mm slice). The 4DCT images resulted in 10 different three-dimensional CT image sets corresponding to different phases of respiratory motion. Average CT image sets were also generated using the 10 4DCT phases for all 3 targets (for comparing with average CBCT).

All the 4DCT and average CT images were imported into a commercially available treatment planning system (TPS) (Eclipse™; Varian Medical Systems). Although visualization of 10 CBCT phases is feasible in the XVI v. 4.5, it does not allow exporting all the 10 phases of CBCT images; therefore, the average CBCT images were exported and used for further comparison.

All images were autoregistered based on pixel data, using a rigid registration algorithm (v. 8.6.15). The volume of target ball was autocontoured using the CT ranger tool available in Eclipse TPS with lower/upper Hounsfield unit (HU) setting −735/+300 HU for average CBCT and average CT and −650/+300 for 4DCT. The lower/upper HU settings used for autosegmentation were optimized to contour all the visible parts of the target (in static image) at lung window level. The 4DCT ITVs were generated by combining all 10-phase target volumes.

The absolute volume difference and centre of mass shift of each average CBCT ITV were measured with respect to corresponding ITVs of 4DCT and average CT. In addition, the spatial overlapping of average CBCT volumes with 4DCT and average CT was evaluated using Dice similarity coefficient[35] which was calculated as shown below:

$$\text{Dice similarity coefficient} = 2 \times \frac{\text{ITV}_{\text{AvgCBCT}} \cap \text{ITV}_{\text{4DCT/AvgCT}}}{\text{ITV}_{\text{AvgCBCT}} + \text{ITV}_{\text{4DCT/AvgCT}}}$$

The ideal value of Dice similarity coefficient is 1; this indicates that both volumes are completely overlapping each other.

Image quality analysis

The image quality of 4DCBCT system was evaluated using Catphan® 600 (The Phantom Laboratory Inc., Salem, NY). This phantom was placed over the QUASAR™ motion platform (Modus Medical Devices Inc., London, ON, Canada) which was programmed to move in CC direction (along the gun-target direction). The sinusoidal respiratory motion (regular) considered for the image quality test has a breathing period of 4 s and CC direction amplitude of 15 mm. Owing to limitations of the motion platform, only one directional motion was considered. 4DCBCT images of the Catphan were acquired for the above-mentioned presets with different gantry rotation speeds. Uniformity and spatial resolution were measured using 4DCBCT images of Catphan in the XVI system, whereas the contrast-to-noise ratio (CNR) was measured using average CBCT images of the dynamic thorax phantom of target size 3 cm diameter in TPS.

Table 1. Internal target volumes (in cubic centimetres) measured with different four-dimensional cone beam CT (4DCBCT) gantry rotation speed

CT	3 cm	2 cm	1 cm
4DCT	44.3	18.4	4.1
4DCT-derived average CT	40.7	17.4	4.0
4DCBCT: 36° min^{-1}	39.5	15.0	3.4
4DCBCT: 50° min^{-1}	39.0	14.7	3.4
4DCBCT: 75° min^{-1}	38.6	14.5	3.2
4DCBCT: 100° min^{-1}	38.2	14.3	3.1
4DCBCT: 150° min^{-1}	37.8	14.2	2.9
4DCBCT: 200° min^{-1}	36.4	14.1	3.0

4DCT, four-dimensional CT.

The CTP486 module of Catphan was used to measure the uniformity. HU values were noted at five different locations (centre, peripheries at top, bottom, left and right) in each 4DCBCT phase, and among the five values, the maximum and minimum values were used to calculate the uniformity by using the following formula:

$$\text{Uniformity} = \frac{(\text{HU}_{\text{Max}} - \text{HU}_{\text{Min}})}{\text{HU}_{\text{Max}}} \times 100$$

Similarly, the spatial resolution [line pairs (lp) per centimetre] was also evaluated qualitatively for each 4DCBCT phase by using the Catphan CTP528 module. Mean and standard deviations were calculated for uniformity and spatial resolution from the 10 values (corresponds to each phase of 4DCBCT).

For CNR measurement, mean HU value of 3-cm target ($\text{MeanHU}_{\text{Target}}$) and background ($\text{MeanHU}_{\text{BKG}}$) were recorded by using a region of interest size 15 × 15 pixels on the average CBCT images of dynamic thorax phantom. Similarly, the standard deviation of the background (STD_{BKG}) was also recorded. The CNR was calculated as follows:

$$\text{CNR} = \frac{\text{MeanHU}_{\text{Target}} - \text{MeanHU}_{\text{BKG}}}{\text{STD}_{\text{BKG}}}$$

RESULTS

Internal target volume analysis

Table 1 shows the measured ITV for various gantry rotation speeds and the target sizes. Figure 1 shows the percentage deviation between the ITVs of average CBCT and 4DCT for various gantry rotation speeds and target sizes. It was observed that the ITV deviation increased with increasing gantry rotation speed. For instance, when comparing the average CBCT ITV with 4DCT ITV, a deviation of −17.8% was observed for 3-cm target at the gantry rotation speed 200° min^{-1}, whereas it was reduced to

Figure 1. The percentage deviations of ITVs of the average 4DCBCT with four-dimensional CT (4DCT) (all 10 phases). 4DCBCT, four-dimensional cone beam CT; dia, diameter; ITV, internal target volume.

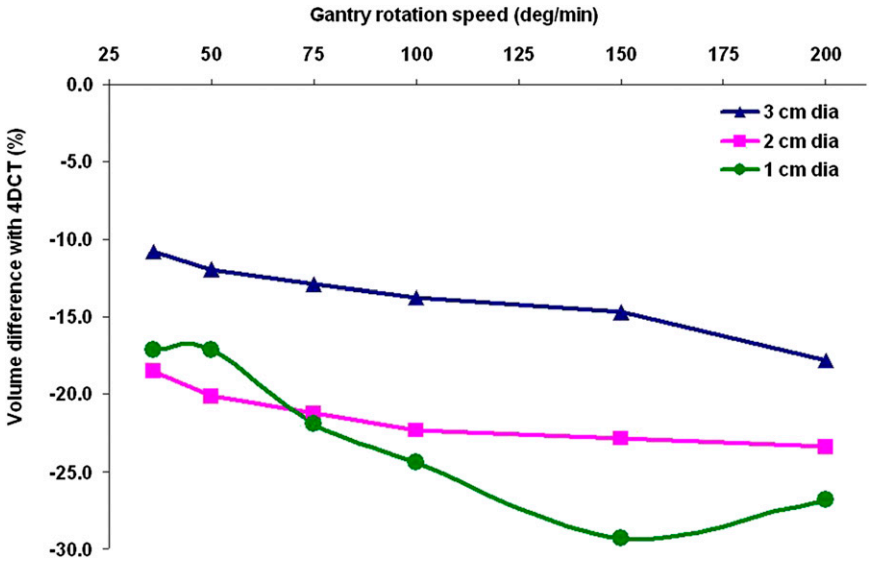

210.8% when using the gantry rotation speed 36° min^{-1}. Among the three target sizes, the maximum deviation was observed for smaller target size *i.e.* 1 cm. For a gantry rotation speed 200° min^{-1}, maximum deviation of −26.8% was observed in the target size 1 cm, whereas it was −17.8% for 3 cm target size.

When comparing the average CBCT with average CT, the deviation was less. Figure 2 shows the percentage deviation between the ITVs of average CBCT and average CT for various gantry rotation speeds and target sizes.

Figure 3 shows Dice similarity coefficient of ITVs of average CBCT, 4DCT and average CT. It was observed that the overlapping volume decreased for increasing gantry rotation speed, and this variation was prominent for 1-cm target size. In addition, the centre of mass shift of all average CBCT ITVs with 4DCT and average CT was observed to be less than a millimetre.

Image quality analysis

Table 2 shows spatial resolution, CNR and uniformity of various gantry rotation speeds. Similar to ITV analysis, the image quality also decreased for increasing gantry rotation speed. For instance, spatial resolution, CNR and uniformity of 4DCBCT scan with gantry rotation speed of 36° min^{-1} were 3.5 ± 0.5 lp cm^{-1}, 67.9 and 2.1 ± 0.2%, respectively, whereas the same parameters of 4DCBCT with gantry rotation speed of 200° min^{-1}

Figure 2. The percentage deviations of ITVs of the average 4DCBCT with average four-dimensional CT-derived ITV. 4DCBCT, four-dimensional cone beam CT; dia, diameter; ITV, internal target volume.

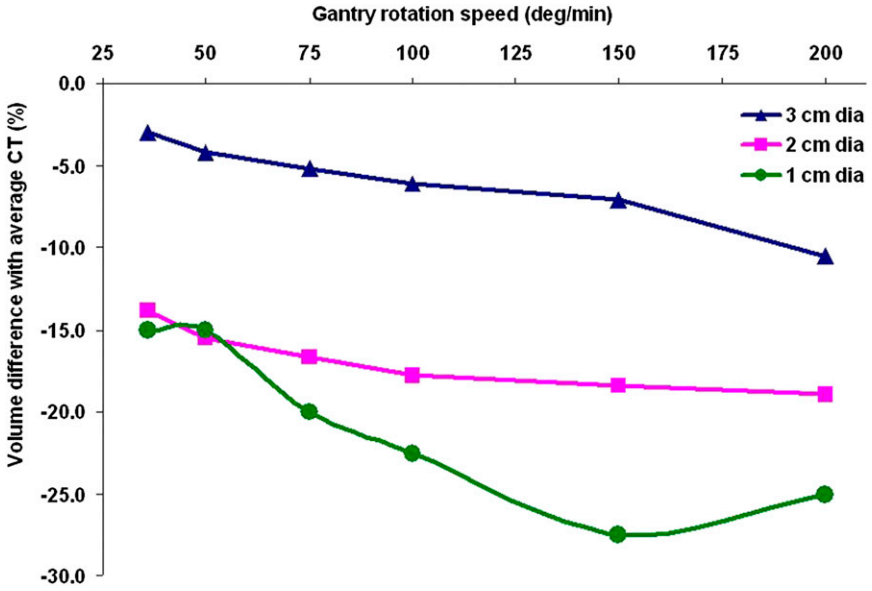

Figure 3. The Dice similarity coefficient of average cone beam CT scans [with four-dimensional CT (4DCT) and average CT] for various gantry rotation speed and target sizes.

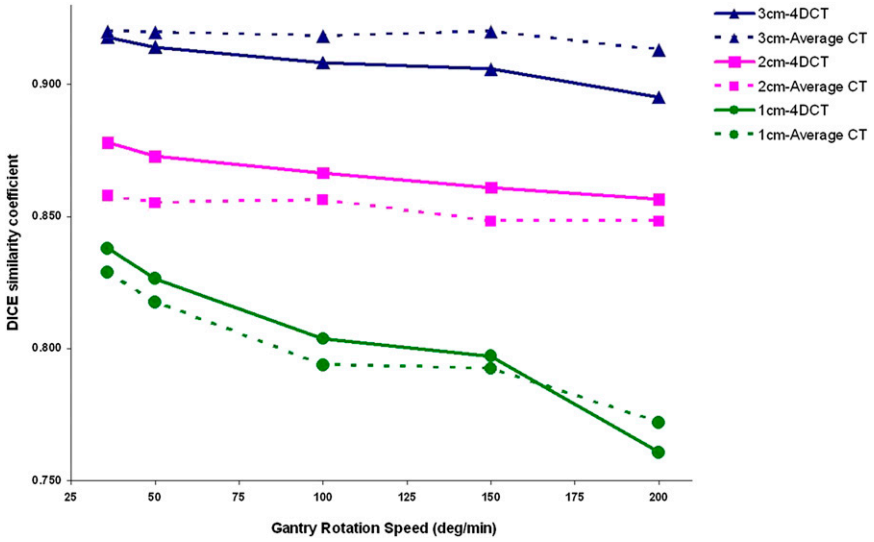

were reduced to $0.8 \pm 1.3\,\mathrm{lp\,cm^{-1}}$, 27.0 and $3.6 \pm 1.8\%$, respectively.

DISCUSSION

The purpose of this study was to evaluate 4DCBCT [Elekta XVI Symmetry™ (Elekta AB)] with different gantry rotation speeds, and the ITV and image quality were used for analysis. ITV deviation increased for increasing 4DCBCT gantry rotation speeds (Tables 1). Similarly, image quality also decreased for increasing gantry rotation speeds (Table 2), and this is in agreement with a previous investigation.[23]

Smaller gantry speed, *i.e.* $36°\,\mathrm{min^{-1}}$ resulted in a less ITV deviation and better image quality than other gantry speeds for all target sizes. This is attributed to the total number of frames acquired in a given 4DCBCT image phase and the total number of frames (F) in a 4DCBCT image acquisition can be calculated as follows;[36]

$$\text{Number of frames (F)} = \frac{\theta_1 - \theta_2}{\omega} \times \Phi$$

or

$$\text{Number of frames (F)} = \text{total scan duration} \times \text{frame rate}$$

where θ_1 and θ_2 are stop and start angle of gantry in a 4DCBCT acquisition, respectively. ω and Φ are gantry rotation speed (in degrees per second) and kilovoltage detector frame rate (frames per second), respectively. Table 3 shows the total number of frames and number of frames per respiratory phase (if we assume 10 respiratory phases for reconstruction) expected for different gantry rotation speeds in 4DCBCT imaging. Alternatively, newer reconstruction methods can also be employed (instead of slow gantry rotation speed) to improve the 4DCBCT image quality with standard gantry rotation speed.[37,38]

The measured ITVs of the average 4DCBCT matched the average 4DCT closer than the 4DCT-derived ITVs (all 10 phases); by contrast, if individual 4DCBCT phases would be used for ITV segmentation, the percentage deviation with 4DCT would be lesser than what we observed in this study. But, the XVI version used in this investigation did not allow exporting all 10 phases of 4DCBCT. Hence, we could only use the average CBCT for evaluation.

The 4DCBCT system has been generally used as a verification imaging tool; alternatively, the system can be used to derive the ITV of moving targets when 4DCT is not available. In such situations, our work will be beneficial for the physicists to understand the uncertainties of 4DCBCT in deriving the ITV.

This investigation has limited itself to a single and regular respiratory motion, whereas the inclusion of more respiratory motion patterns would be useful to understand the influence of respiratory motion in the 4DCBCT acquisition. The influence of breathing period on 4DCBCT image quality has been previously

Table 2. Image quality of four-dimensional cone beam CT images acquired at different gantry rotation speed

Gantry speed ($°\,\mathrm{min^{-1}}$)	Spatial resolution ($\mathrm{lp\,cm^{-1}}$)	CNR	Uniformity (%)
36	3.5 ± 0.5	67.9	2.1 ± 0.2
50	2.6 ± 0.5	55.7	2.2 ± 0.7
75	2.7 ± 1.2	55.6	2.7 ± 0.3
100	1.6 ± 1.5	56.7	2.9 ± 0.3
150	1.5 ± 1.6	46.0	3.2 ± 1.1
200	0.8 ± 1.3	27.0	3.6 ± 1.8

CNR, contrast-to-noise ratio; lp, line pairs.

Table 3. Total number of frames and number of frames per respiratory phase expected in a four-dimensional cone beam CT acquisition with different gantry rotation speed

Gantry speed (° min^{-1})	Total number of frames	Number of frames per phase[a]
36	1833	183.3
50	1320	132.0
75	880	88.0
100	660	66.0
150	440	44.0
200	330	33.0

[a]Assuming 10 respiratory phases for reconstruction.

reported.[23] It was found that for a fixed amplitude, increasing the breathing period decreased the image quality because the number of respiratory cycles that can be covered by a given 4DCBCT scan would be reduced. This respiratory motion effect in 4DCBCT is the opposite of that in 4DCT imaging where the ITV deviation was observed to be increased for increasing target motion velocity.[39] Hence, to achieve an optimal image quality, the total 4DCBCT scan duration has to be adjusted according to the respiration period by altering the parameters such as gantry rotation speed and gantry start–stop angles, *i.e.* the total scan duration should be increased for long breathing period and *vice versa*.

This study evaluated only the effect of 4DCBCT gantry rotation speed (with constant tube current) on ITV and image quality, and its effect on patient dose is beyond the scope of this work. The radiation exposure in a 4DCBCT scan which has a slow gantry rotation speed would increase, and it can be minimized by reducing the tube current.[23] Lastly, the presented results are specific to the window level threshold used in this study, and this should be considered when interpreting the results.

CONCLUSION

A 4DCBCT system was evaluated with different gantry rotation speeds. Increasing the gantry rotation speed increased the 4DCBCT average ITV deviation from the 4DCT- (all 10 phases) and average 4DCT-derived ITVs. In addition, the increasing gantry rotation speed decreased the image quality of the 4DCBCT system. Therefore, the impact of gantry rotation speed has to be considered when using the 4DCBCT for ITV definition.

FUNDING

This work was supported by the Department of Science and Technology, Government of India, grant no: IR/SO/LS 02/2003.

REFERENCES

1. Galvin JM, De Neve W. Intensity modulating and other radiation therapy devices for dose painting. *J Clin Oncol* 2007; **25**: 924–30. doi: http://dx.doi.org/10.1200/JCO.2007.10.6716
2. Bortfeld T, Jokivarsi K, Goitein M, Kung J, Jiang SB. Effects of intra-fraction motion on IMRT dose delivery: statistical analysis and simulation. *Phys Med Biol* 2002; **47**: 2203–20. doi: http://dx.doi.org/10.1088/0031-9155/47/13/302
3. Yoganathan SA, Maria Das KJ, Kumar S. Computational model to simulate the interplay effect in dynamic IMRT delivery. *Int J Phys Conf Ser* 2014; **489**: 12042–47. doi: http://dx.doi.org/10.1088/1742-6596/489/1/012042
4. Das KJ, Agarwal A, Yoganathan SA, Raj DG, Kumar S. Investigation of inter and intra-fractional uncertainties in lung IMRT delivery. In World Congress on Medical Physics and Biomedical Engineering. *IFBME Proc* 2013; **39**: 1857–59.
5. International Commission on Radiation Units and Measurements. *Prescribing, recording and reporting photon beam therapy. Supplement to report 50. Report 62*. Washington, DC: ICRU; 1999.
6. Hugo GD, Yan D, Liang J. Population and patient-specific target margins for 4D adaptive radiotherapy to account for intra-and inter-fraction variation in lung tumour position. *Phys Med Biol* 2007; **52**: 257–74. doi: http://dx.doi.org/10.1088/0031-9155/52/1/017
7. Wong JW, Sharpe MB, Jaffray DA, Kini VR, Robertson JM, Stromberg JS, et al. The use of active breathing control (ABC) to reduce margin for breathing motion. *Int J Radiat Oncol Biol Phys* 1999; **44**: 911–19. doi: http://dx.doi.org/10.1016/S0360-3016(99)00056-5
8. Ohara K, Okumura T, Akisada M, Inada T, Mori T, Yokota H, et al. Irradiation synchronized with respiration gate. *Int J Radiat Oncol Biol Phys* 1989; **17**: 853–57. doi: http://dx.doi.org/10.1016/0360-3016(89)90078-3
9. Yoganathan SA, Das KJ, Raj DG, Kumar S. Dosimetric verification of gated delivery of electron beams using a 2D ion chamber array. *J Med Phys* 2015; **40**: 68–73. doi: http://dx.doi.org/10.4103/0971-6203.158671
10. Keal PJ, Kini VR, Vedam SS, Mohan R. Motion adaptive X-ray therapy: a feasibility study. *Phys Med Biol* 2001; **46**: 1–10.
11. Yoganathan SA, Das KJ, Agarwal A, Kumar SKS, Velmurugan J, Kumar S. Synchronization of intra-fractional motion in dynamic IMRT delivery. In World Congress on Medical Physics and Biomedical Engineering. *IFBME Proc* 2013; **39**: 1923–25.
12. Yoganathan SA, Maria Das KJ, Agarwal A, Kumar S. Performance evaluation of respiratory motion-synchronized dynamic IMRT delivery. *J Appl Clin Med Phys* 2013; **14**: 4103. doi: http://dx.doi.org/10.1120/jacmp.v14i3.4103
13. Jaffray DA, Siewerdsen JH, Wong JW, Martinez AA. Flat-panel cone-beam computed tomography for image-guided radiation therapy. *Int J Radiat Oncol Biol Phys*. 2002; **53**: 1337–49. doi: http://dx.doi.org/10.1016/S0360-3016(02)02884-5
14. Grills IS, Hugo G, Kestin LL, Galerani AP, Chao KK, Wloch J, et al. Image-guided radiotherapy *via* daily online cone-beam CT substantially reduces margin requirements for stereotactic lung radiotherapy. *Int J Radiat Oncol Biol Phys* 2008; **70**: 1045–56. doi: http://dx.doi.org/10.1016/j.ijrobp.2007.07.2352
15. Yeung AR, Li JG, Shi W, Newlin HE, Chvetsov A, Liu C, et al. Tumor localization using cone-beam CT reduces setup margins in conventionally fractionated radiotherapy for lung tumors. *Int J Radiat Oncol Biol Phys* 2009; **74**: 1100–07. doi: http://dx.doi.org/10.1016/j.ijrobp.2008.09.048

16. Nijkamp J, Pos FJ, Nuver TT, de Jong R, Remeijer P, Sonke JJ, et al. Adaptive radiotherapy for prostate cancer using kilovoltage cone-beam computed tomography: first clinical results. *Int J Radiat Oncol Biol Phys* 2008; **70**: 75–82. doi: http://dx.doi.org/10.1016/j.ijrobp.2007.05.046
17. Zhang Q, Hu YC, Liu F, Goodman K, Rosenzweig KE, Mageras GS. Correction of motion artifacts in cone-beam CT using a patient-specific respiratory motion model. *Med Phys* 2010; **37**: 2901–09. doi: http://dx.doi.org/10.1118/1.3397460
18. Yang Y, Schreibmann E, Li T, Xing L. Motion correction for improved target localization with on-board cone-beam computed tomography. *Phys Med Biol* 2006; **51**: 253–67. doi: http://dx.doi.org/10.1088/0031-9155/51/2/005
19. Aibe N, Yamazaki H, Nishimura T, Oota Y, Iwama K, Nakamura S, et al. Analysis of intrafractional organ motion by megavoltage computed tomography in patients with lung cancer treated with image-guided stereotactic body radiotherapy using helical tomotherapy. *Anticancer Res* 2014; **34**: 7383–88.
20. Descovich M, McGuinness C, Kannarunimit D, Chen J, Pinnaduwage D, Pouliot J, et al. Comparison between target margins derived from 4DCT scans and real-time tumor motion tracking: Insights from lung tumor patients treated with robotic radiosurgery. *Med Phys* 2015; **42**: 1280–87. doi: http://dx.doi.org/10.1118/1.4907956
21. Cai W, Hurwitz MH, Williams CL, Dhou S, Berbeco RI, Seco J, et al. 3D delivered dose assessment using a 4DCT-based motion model. *Med Phys* 2015; **42**: 2897–907. doi: http://dx.doi.org/10.1118/1.4921041
22. Li T, Xing L, Munro P, McGuinness C, Chao M, Yang Y, et al. Four-dimensional cone-beam computed tomography using an on-board imager. *Med Phys* 2006; **33**: 3825–33. doi: http://dx.doi.org/10.1118/1.2349692
23. Li T, Xing L. Optimizing 4D cone-beam CT acquisition protocol for external beam radiotherapy. *Int J Radiat Oncol Biol Phys* 2007; **67**: 1211–19. doi: http://dx.doi.org/10.1016/j.ijrobp.2006.10.024
24. Sonke JJ, Zijp L, Remeijer P, van Herk M. Respiratory correlated cone beam CT. *Med Phys* 2005; **32**: 1176–86. doi: http://dx.doi.org/10.1118/1.1869074
25. Lu J, Guerrero TM, Munro P, Jeung A, Chi PC, Balter P, et al. Four-dimensional cone beam CT with adaptive gantry rotation and adaptive data sampling. *Med Phys* 2007; **34**: 3520–29. doi: http://dx.doi.org/10.1118/1.2767145
26. Shieh CC, Kipritidis J, O'Brien RT, Cooper BJ, Kuncic Z, Keall PJ. Improving thoracic four-dimensional cone-beam CT reconstruction with anatomical-adaptive image regularization (AAIR). *Phys Med Biol* 2015; **60**: 841–68. doi: http://dx.doi.org/10.1088/0031-9155/60/2/841
27. Li J, Harrison A, Yu Y, Xiao Y, Werner-Wasik M, Lu B. Evaluation of Elekta 4D cone beam CT-based automatic image registration for radiation treatment of lung cancer. *Br J Radiol* 2015; **88**: 20140620. doi: http://dx.doi.org/10.1259/bjr.20140620
28. Kipritidis J, Hugo G, Weiss E, Williamson J, Keall PJ. Measuring interfraction and intrafraction lung function changes during radiation therapy using four-dimensional cone beam CT ventilation imaging. *Med Phys* 2015; **42**: 1255–67. doi: http://dx.doi.org/10.1118/1.4907991
29. Dhou S, Hurwitz M, Mishra P, Cai W, Rottmann J, Li R, et al. 3D fluoroscopic image estimation using patient-specific 4DCBCT-based motion models. *Phys Med Biol* 2015; **60**: 3807–24. doi: http://dx.doi.org/10.1088/0031-9155/60/9/3807
30. Takahashi W, Yamashita H, Kida S, Masutani Y, Sakumi A, Ohtomo K, et al. Verification of planning target volume settings in volumetric modulated arc therapy for stereotactic body radiation therapy by using in-treatment 4-Dimensional cone beam computed tomography. *Int J Radiat Oncol Biol Phys* 2013; **86**: 426–31. doi: http://dx.doi.org/10.1016/j.ijrobp.2013.02.019
31. Vergalasova I, Maurer J, Yin FF. Potential underestimation of the internal target volume (ITV) from free-breathing CBCT. *Med Phys* 2011; **38**: 4689–99. doi: http://dx.doi.org/10.1118/1.3613153
32. Clements N, Kron T, Franich R, Dunn L, Roxby P, Aarons Y, et al. The effect of irregular breathing patterns on internal target volumes in four-dimensional CT and cone-beam CT images in the context of stereotactic lung radiotherapy. *Med Phys* 2013; **40**: 021904. doi: http://dx.doi.org/10.1118/1.4773310
33. Liao Y, Turian J, Templeton A, Redler G, Chu J. SU-E-J-35: using CBCT as the alternative method of assessing ITV volume. *Med Phys* 2015; **42**: 3271. doi: http://dx.doi.org/10.1118/1.4924122
34. Seppenwoolde Y, Shirato H, Kitamura K, Shimizu S, van Herk M, Lebesque JV, et al. Precise and real-time measurement of 3D tumour motion in lung due to breathing and heartbeat, measured during radiotherapy. *Int J Radiat Oncol Biol Phys* 2002; **53**: 822–34. doi: http://dx.doi.org/10.1016/S0360-3016(02)02803-1
35. Dice LR. Measures of the amount of ecologic association between species. *Ecology* 1945; **26**: 297–302. doi: http://dx.doi.org/10.2307/1932409
36. Elekta Limited. *Instructions for use—XVI R4.5 (Document ID: 1502627_01)*. Crawley, UK: Elekta Limited; 2013.
37. Jia X, Tian Z, Lou Y, Sonke JJ, Jiang SB. Four-dimensional cone beam CT reconstruction and enhancement using a temporal nonlocal means method. *Med Phys* 2012; **39**: 5592–602. doi: http://dx.doi.org/10.1118/1.4745559
38. Yan H, Zhen X, Folkerts M, Li Y, Pan T, Cervino L, et al. A hybrid reconstruction algorithm for fast and accurte 4D cone-beam CT imaging. *Med Phys* 2014; **41**: 071903. doi: http://dx.doi.org/10.1118/1.4881326
39. Nakamura M, Narita Y, Sawada A, Matsugi K, Nakata M, Matsuo Y, et al. Impact of motion velocity on four-dimensional target volumes: a phantom study. *Med Phys* 2009; **36**: 1610–17. doi: http://dx.doi.org/10.1118/1.3110073